Vanadium sesquioxide-polymer composites: the study of electrical conductivity

YI PAN, GUO ZHANG WU, XIAO SU YI
Department of Materials Science and Engineering, Zhejiang University, Hangzhou 310027, People's Republic of China

The electrical conductivity of V_2O_3-polymer composites were studied by examining the dependence of resistivity (conductivity) on the volume fraction of V_2O_3. The experimental data (ρ_m versus ϕ) were fitted (using a computer program) to the GEM equation with satisfactory accuracy. The critical volume fraction and other parameters evaluated by fitting (t, σ_h and σ_c) and calculated after fitting L_ϕ and m_ϕ, L_f and m_f were analysed by taking into account the geometry, orientation and arrangement of the two components. The physical meanings of L, m and t are further illustrated on the basis of their definitions.

1. Introduction

Conductive polymer composites (CPC) made by incorporating different volume fractions of conductive powders into a polymer matrix exhibit an extremely wide range of electrical resistivities (from 10^{-3} to $10^{16} \, \Omega \, cm$) [1]. They have been used for various purposes, such as electrostatic dissipation (ESD), electromagnetic interference shielding (EMIS) and self-limit heaters, etc. [1]. Conductive polymer composite material is usually very flexible, it can be soft or stiff, its formation is quite steady and, most importantly, its resistivity is adjustable. Moreover, the temperature dependence of resistivity at some temperatures behaves with an extremely large positive temperature coefficient (PTC), making CPC potential thermistor materials. The conductive fillers are mainly carbon black, metal powders and powders of transition metal oxides, and the matrices involve many conventional polymers, including both thermoplastic and thermoset.

The electrical resistivity of CPCs is a function of the volume fraction of the conductive filler, and is also affected by intrinsic properties, e.g. geometry (particle sizes and shapes) and the arrangement of both components. When other conditions are fixed, the resistivity is a reducing function of the filler volume fraction. It reduces as the volume fraction increases, slightly at first and then abruptly when the critical volume fraction is reached, i.e. an insulator to conductor transition takes place. A further increase in the volume fraction results in a slight decrease in resistivity.

The insulator to conductor transition, which occurs at the critical volume fraction, implies that the percolation path formed by the conductive filler particles just crosses the composite medium. Therefore, the strong dependence of resistivity upon volume fraction around the critical volume fraction can be described by the percolation theory. The critical volume fraction thus corresponds to the percolation threshold [2].

The influence on electrical properties of various factors other than volume fraction may be examined by their influence on the critical volume fraction. This topic can be traced back 100 years, however, in recent years interest has been renewed because of the needs of the design of composites and the development of smart materials. The smartness of CPCs can be illustrated by their extremely large PTC anomaly of electrical resistivity. It has been reported that CPCs with carbon black, metal powder or some transition metal oxide incorporated all exhibit the PTC effect to different extents at the temperature close to the melting points of polymer matrices [3].

Vanadium suboxide-polymer composites are a new category of CPC. Hu *et al.* [4] reported on the PTC effect of such materials. Pan *et al.* [5] also reported that V_2, O_3 and VO_2 incorporated into various brands of polyethylenes showed PTC anomalies as large as 7-9 orders of magnitudes of electrical resistivities at temperatures of 85, 103 and 115 °C, respectively. It became necessary to investigate the room temperature resistivity of vanadium suboxide-polymer systems by taking into account the volume fraction, the intrinsic property and the arrangement of the components within the composite. This paper is to report the work on this group, concerning this topic.

The study followed previous work done by Bruggeman [6], Landauer [7] and McLachlan [8], in which so-called macroscopic mixtures of insulators and conductors were dealt with. According to the arrangement of the two components in the mixture, asymmetric and symmetric effective medium equations were introduced for the cases where one component was coated by the other (host) and two components were unidentified in both geometry and arrangement. An intermediate effective medium equation was also introduced to deal with the case between the above two cases. The percolation mode was also presented as far as the resistivity change near the critical volume frac-

tion was concerned. After summarizing the equations and modes for various special cases, McLachlan [8] suggested a general effective medium (GEM) equation, in which the conductivity of medium and the volume fraction were contained in an implicit function with no special assumptions for the geometry or arrangement manner of the components. Various parameters involving critical volume fraction, original properties and geometrical features of components characterize the change manner of medium conductivity with the volume fraction.

V_2O_3–polymer composites were made by incorporating V_2O_3 powders into polymer matrices by shear milling, compaction sinter moulding, or mixing and casting. The conductivity versus volume fraction was measured and the experimental data were fitted by a computer program to the GEM equation. The critical volume fraction, as well as other variable parameters, were obtained directly by fitting and by calculation after fitting. The critical volume fraction and the physical meanings of these parameters were analysed and discussed by considering the particle size and shape, the mixing method and the interactions between components. Further understanding of these parameters on the basis of their definitions were presented giving greater significance to the GEM equation.

2. Theories and equations

In the process of studying physical properties of multiphase mixtures various models have been given to describe the dependence of physical properties, such as Young's modulus, the dielectric constant or electrical conductivity, upon the relative concentration (volume fraction). Each of them may fit only a special case, in which strict assumptions are made. McLachlan [8] postulated a GEM equation after studying and summarizing various previous works. As far as the conductivity of a binary system is concerned, the GEM equation is written as

$$\frac{f(\sigma_l^{1/t} - \sigma^{1/t})}{\sigma_l^{1/t} + A\,\sigma^{1/t}} + \frac{\phi(\sigma_h^{1/t} - \sigma_m^{1/t})}{\sigma_h^{1/t} + A\,\sigma_m^{1/t}} = 0 \qquad (1)$$

where σ_m, σ_l and σ_h are the conductivities of medium-, low- and high-conductivity components, respectively, f and ϕ are volume fractons of low- and high-conductivity components, respectively, and $f + \phi = 1$ always holds. A is defined as

$$A = \frac{1 - \phi_c}{\phi_c} = \frac{f_c}{1 - f_c} \qquad (2)$$

ϕ_c ($= 1 - f_c$) is the critical volume fraction of the high-conductivity component, at which the insulator to conductor transition occurs. ϕ_c is related to the geometries and orientations of both components according to

$$\phi_c = L_\phi/(1 - L_f + L_\phi)$$

(oriented ellipsoids) \qquad (3a)

$$\phi_c = m_f/(m_f + m_\phi)$$

(random ellipsoids) \qquad (3b)

where L_ϕ and L_f are demagnetization constants of high- and low-conductivity component particles, respectively. As the particle shape is spherical, L is 1/3. If the component is fibre- or layer-shaped and is oriented in the electric current direction across the medium $L = 0$, perpendicular to the current $L = 1$. L stands for the combination of particle shape and orientation to applied field. m_ϕ and m_f are parameters for a random case. Actually, effective L is often used, even in random cases. Exponent t is defined by the following equations

$$t = 1/(1 - L_f + L_\phi)$$

(oriented ellipsoids) \qquad (4a)

$$t = (m_f\,m_\phi)/(m_f + m_\phi)$$

(random ellipsoids) \qquad (4b)

Consequently, L and m may be related by the following equations

$$L_\phi = \phi_c/t \qquad (5a)$$

$$L_f = 1 - [(1 - \phi_c)/t] \qquad (5b)$$

$$m_\phi = t/\phi_c \qquad (6a)$$

$$m_f = t/(1 - \phi_c) \qquad (6b)$$

The GEM equation gives complete information on how the volume fraction affects the medium conductivity by taking into account the intrinsic conductivities, geometries, arrangement and the orientations to the applied electric fields of both components. It has been assumed in introducing the GEM equation that: (1) the binary system is macroscopically homogeneous; (2) the particle size distributions are infinitely wide and that they are in contact with each other, with no voids remaining; (3) the electrical contact potential between like and unlike particles are negligible.

If two components are identical in geometry and arrangement (symmetric case), $L_\phi = L_f = L$ and $t = 1$, Equation 1 then becomes

$$\frac{(1 - \phi)(\sigma_l - \sigma_m)}{\sigma_l + \left(\dfrac{1 - L}{L}\right)\sigma_m} + \frac{\phi(\sigma_h - \sigma_m)}{\sigma_h + [(1 - L/L)\sigma_m]} = 0 \qquad (7)$$

which is Bruggeman's symmetric equation [6].

For the case where $\sigma_l = 0$ (conductor host) or $\rho_l = 0$ (insulator host) the GEM equations may be reduced to be

$$\sigma_m = \sigma_h \left(1 - \frac{f}{f_c}\right)^{m_f f_c}$$

(conductor host) \qquad (8)

$$\rho_m = \rho_h (1 - \phi/\phi_c)^{m_\phi \phi_c}$$

(insulator host) \qquad (9)

Equations 8 and 9 have the mathematical form of the percolation theory. The GEM equation can also be reduced by some assumptions to equations similar to those introduced from various other models.

3. Experiments and computer fittings

3.1. Raw materials

V_2O_3 powder was prepared via reduction of V_2O_5 (chemically pure; Shanghai Chemical Agent Co.) at a high temperature in a hydrogen atmosphere. X-ray diffraction (XRD) and thermal gravity analysis (TGA) were used to determine whether or not the reduced product was pure and stoichiometric. Some batches of V_2O_3 powder were further ball-milled. The particle sizes of as-produced and ball-milled V_2O_3 were measured using a laser droplet analyser, they were 5.96 and 1.66 μm, respectively. The specific gravity of V_2O_3 was estimated as $4.87\,\mathrm{g\,cm^{-3}}$, the same as that of V_2O_3 single crystals. The electrical resistivities of dense compacts of as-produced and ball-milled V_2O_3 were measured using the collinear four-probe array method. The values of 3.7×10^{-2} and $9.2 \times 10^{-2}\,\Omega\,\mathrm{cm}$ were taken as ρ_l or σ_h in the GEM equation.

The polymer materials used as matrices in the composites were HDPE, LLDPE, LDPE, PVC and epoxy. They were all Chinese domestic. General information about these materials are listed in Table I.

3.2. Sample preparations

For the samples with LDPE, LLDPE or LDPE as matrix, the incorporation of V_2O_3 into the polymer was completed by shear milling at 140–180 °C for more than 20 min. The milled pieces were then hot-pressed under $800\,\mathrm{kg\,cm^{-2}}$ at the same temperature into bars $20 \times 5 \times 1$ mm. The press direction was perpendicular to the shear.

For the samples with PVC powder as matrix, V_2O_3 and PVC powders were first dry blended and then hot-pressed into discs at a relatively low temperature (50 °C) so that the arrangement was compaction sinter moulded.

For the samples with epoxy as matrix, a paste of V_2O_3 and epoxy was cast. The paste was first cured at 80 °C in vacuum for 0.5 h, and then pressed under 1.013×10^7 Pa for 3 min followed by further curing at 80 °C for 8 h. The process may have prevented air pores forming.

The volume fractions were determined by simple weighing before mixing. V_2O_3 powder was gradually added during shear milling.

3.3. Resistivity measurements

Room temperature resistivities of $< 10^5\,\Omega\,\mathrm{cm}$, were measured using the collinear four-probe array method (STZ 8501; made in the National Key Lab of Semiconductor Materials, Zhejiang University). Resistivities $> 10^5\,\Omega\,\mathrm{cm}$, up to $10^{17}\,\Omega\,\mathrm{cm}$, were measured using a three-probe array (2C36), in which an electric current as low as 10 A could be measured. The resistivity versus volume fraction was then plotted, Figs 1–4. Each point in the figures was an average value of at least ten samples, the standard deviation was always small enough to be negligible.

3.4. Computer fittings

The experimental data for each system was fitted to the GEM equation by computer programming. The GEM equation may be written in another form

$$\phi = B + C\,P_m + D/P_m \qquad (10)$$

where B, C and D are functions of ρ_l, ρ_h and ϕ_c; $P = \sigma_x^{1/t}$, where x represents l, h or m.

$$B = 1/(1 + A) \qquad (10a)$$

$$C = A/[P_h(1 + A)] \qquad (10b)$$

$$D = (-P_h P_l)/[P_h(1 + A)] \qquad (10c)$$

where ϕ and A are as above.

A function S may be defined as

$$S = \sum_{}^{n} (\phi - \phi_E)^2 \qquad (11)$$

where n is the number of experimental data points, ϕ_E, experimental volume fraction. For the best fit the following equations have to be satisfied

$$\frac{\partial S}{\partial a_j} = 0 \qquad (12)$$

where a represents B, C or D. After arbitrarily giving a value of t and solving the equation series of Equation 12 by computer, B, C and D were calculated and σ_l, σ_h and ϕ_c were then estimated. The final solutions of σ_l, σ_h and ϕ_c were determined after the correct t value was chosen. The t value was modified until

$$\delta = [S/(n - p)]^{1/2} \qquad (13)$$

was limited to the smallest possible value. Equation 13 was used to estimate the error of the computer fitting. Here S and n were defined as previously, p is the number of fitting parameters. The whole process is called four-parameter fitting. The curves obtained through four-parameter fitting were also shown in Figs 1–4.

It was often found that four-parameter fitting led to a large fluctuation in σ_h. Therefore, three-parameter fitting (σ_h was given a reasonable value) was performed for all systems. The results of four-parameter

TABLE I Polymers used as matrices

Name	Type	Density (g cm^{-3})	T_m/T_g	Company
HDPE	2480	0.941–0.947	130	Qilu
LLDPE	DFDA7042	0.918–0.922	104	Qilu
LDPE	ER2A	0.92	90	Yianshan
PVC	(Powder)	1.46	82	Jilin Univ.
Epoxy	6101	1.25	–	Shanghai

TABLE II Four-parameter fitting

Sample	σ_l^{-1} (Ω cm)	σ_h^{-1} (Ω cm)	t	ϕ_c	L_ϕ	m_ϕ	L_f	m_f	δ (%)
HDPE1	3.65×10^{10}	2.51×10^{-2}	2.38	0.29	0.124	8.04	0.702	3.35	2.4
LLDPE1	3.31×10^{10}	0.703	1.00	0.33	0.333	3.00	0.333	1.49	1.9
LDPE1	2.58×10^{12}	0.138	2.02	0.38	0.187	5.34	0.693	3.26	2.3
EPOXY1	2.38×10^{12}	0.300	1.70	0.20	0.118	8.50	0.592	2.12	3.0
PVC1	2.41×10^{12}	0.308	1.52	0.11	0.072	13.8	0.414	1.71	1.1
HDPE2	1.47×10^{10}	0.176	1.78	0.28	0.159	6.28	0.596	2.47	1.2
LLDPE2	8.85×10^{10}	3.96×10^{-2}	3.24	0.32	0.098	10.2	0.790	4.76	1.5

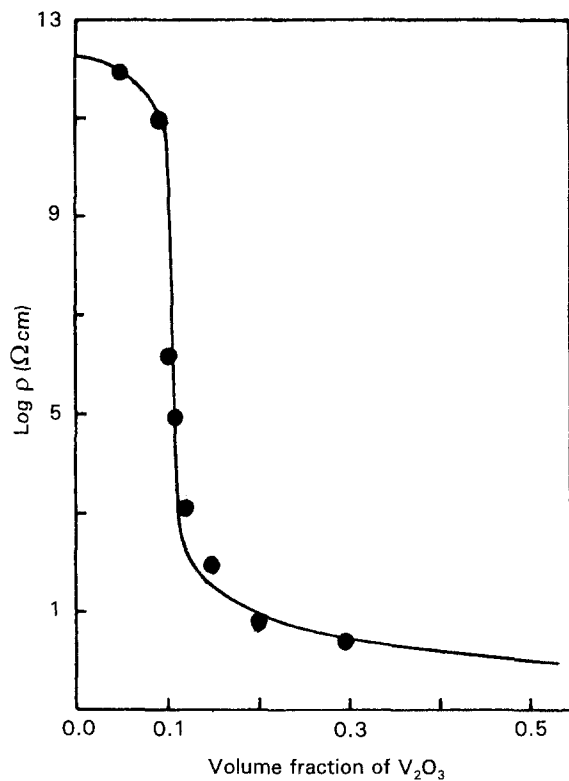Note: The sample is named by the matrix material and a number, 1 = as-produced V_2O_3, 2 = ball-milled V_2O_3.

Figure 1 Resistivity versus volume fraction of V_2O_3–PVC composite.

Figure 2 Resistivity versus volume fraction of V_2O_3–HDPE composite. ●—●, as-produced; ▲—▲, ball-milled.

and three-parameter fittings are listed in Tables II and III, respectively.

3.5. SEM studies of particle geometry and morphology

For illustrative purposes the particles of as-produced and ball-milled V_2O_3 powders were observed and the morphologies of composites showing the arrangements of the two components were observed by SEM, the micrographs obtained are shown in Figs 6 and 7.

4. Results and discussion

The resistivity versus volume fraction for the V_2O_3–PVC composite made by compaction sinter moulding is shown in Fig. 1. The particle size ratio of PVC to V_2O_3 was about 14. The resistivity fell abruptly from 10^{12} to 10^2 Ω cm at a V_2O_3 volume fraction of about 0.1. The critical volume fraction was then determined to be 0.1. Kusy [9] and Bhattacharya
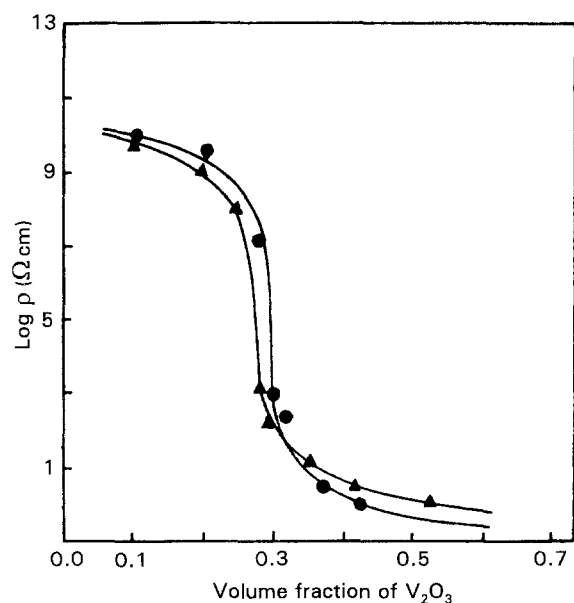
[10] studied macroscopic mixtures of metal powders and polymer particles; independently they suggested two equations relating the particle size ratio to the critical volume fraction by taking into account the component arrangement (coordinate number). Kusy's and Bhattacharya's equation results are plotted in Fig. 5. The results of these experiments ($R_p/R_m = 14$, $\phi_c = 0.1$) are also marked on the figure. It can be seen that our result fell between Kusy's and Battacharya's predictions, but closer to Kusy's. This may indicate that cubic packing (more random) of PVC particles was predominant.

Figs 2 and 3 show the resistivity versus volume fraction of V_2O_3 in HDPE and LLDPE matrices, respectively. The computer fitted curves ran perfectly through most of the experimental data points. One interesting thing to be noted is that ball-milled V_2O_3 gave smaller critical volume fractions and lower resistivity decreasing rates. This may suggest that finer filler favours the formation of an electrical percolation network across the medium and forms more branches within the network. The critical volume fraction was about 0.3. Other parameters, σ_l, σ_h and t, are listed in Tables II and III.

Fig. 4 shows the comparison of ρ_m–ϕ relations of as-produced V_2O_3 incorporated into LDPE, HDPE and epoxy. The same filler in different matrices gave
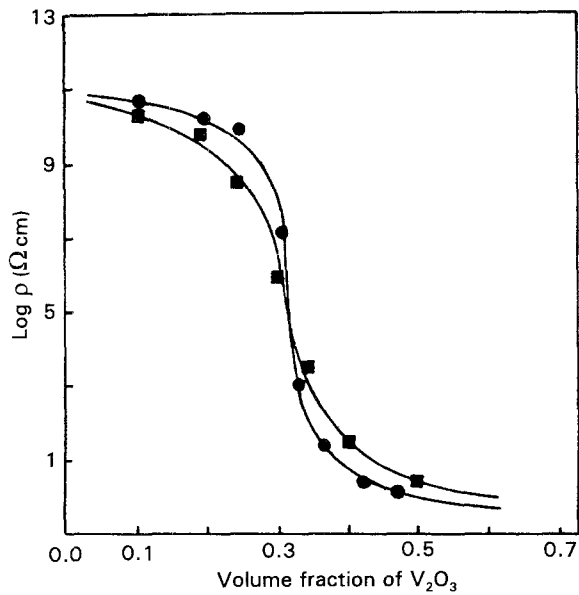
Figure 3 Resistivity versus volume fraction of V_2O_3–LLDPE composite. ●—●, as-produced; ■—■, ball-milled.
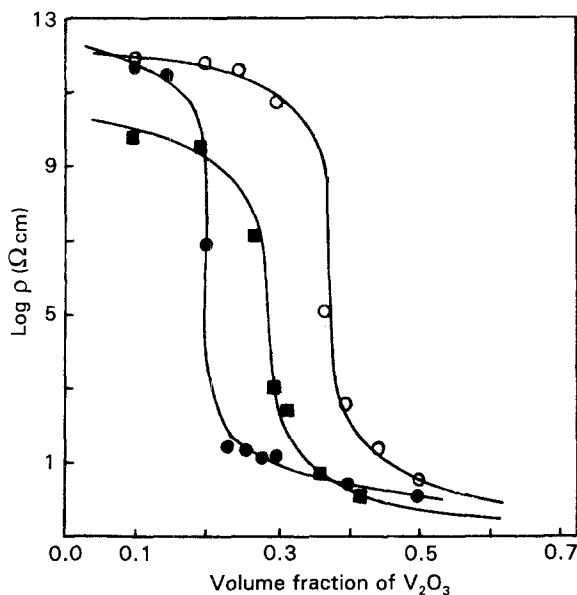

Figure 4 Comparison of resistivity versus volume fraction of V_2O_3–HDPE (■—■), V_2O_3–LDPE (○—○) and V_2O_3–Epoxy (●—●).

different critical volume fractions. This is explained in a later section.

Computer fitting experimental data to the GEM equation gave all the variable parameters listed in Tables II and III. Most values of L_0 (effective demagnetization constant of V_2O_3) were smaller than 1/3, suggesting that the dimension of V_2O_3 particles along the electric current (perpendicular to the pressing direction during formation) was longer than that in other directions. The micrographs shown in Fig. 6 were taken from as-produced and ball-milled V_2O_3 powders. A dimension difference of about 5:1 (aspect ratio) could be seen in the as-produced V_2O_3 powder. The rod- and long flake-shaped particles lying in the electric current plane perpendicular to the press direction are shown in Fig. 7a. L_ϕ values smaller than 1/3 is in agreement with this fact.
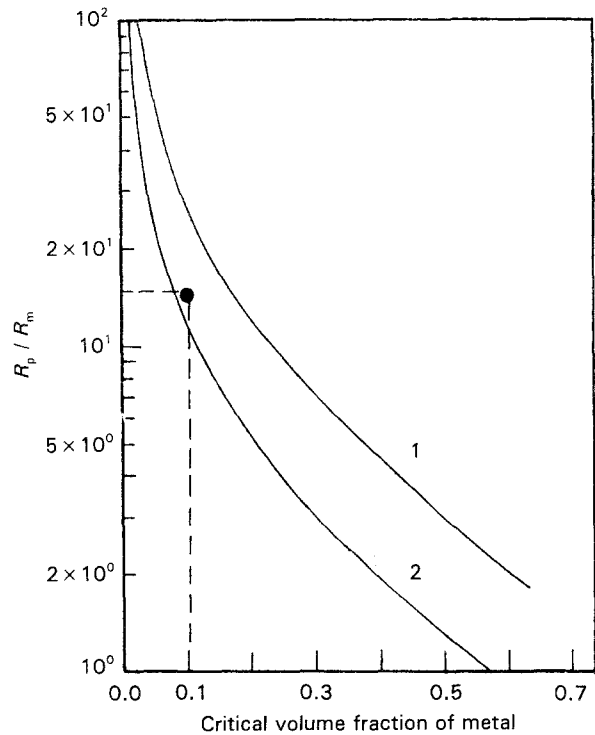

Figure 5 R_p/R_m versus ϕ_c of V_2O_3–PVC: Kusy's model, 1; Bhattacharya 2; Kusy; ●, result from the present work.

In Tables II and III it is shown that V_2O_3 powder treated and mixed in the same way in different matrices gave different t and ϕ_c values, but similar values of L_ϕ and m_ϕ, particularly in three-parameter fitting (Table III). For as-produced V_2O_3 incorporated into HDPE, LLDPE, LDPE and epoxy, L_ϕ was 0.136 ± 0.002 and m_ϕ was 7.37 ± 0.12. For ball-milled V_2O_3 incorporated into HDPE and LLDPE, L_ϕ was 0.12 ± 0.00 and m_ϕ was 8.36 ± 0.04. This phenomenon has helped in further understanding of the meanings of L_ϕ and m_ϕ. According to definition, L is a parameter determined solely by the geometry and the orientation to the applied field of the filler particles. In the case of as-produced V_2O_3, L_ϕ and m_ϕ were determined only by the individual particles with an aspect ratio of 5:1 lying in the electric current plane, which can be seen in Fig. 7a. In the case of ball-milled V_2O_3, L_ϕ, which would have been larger than in the former case since the particles were uniaxial after ball-milling, was actually smaller than L_ϕ in the former case. This can be explained only by the fine V_2O_3 formed flaky aggregates lying in the electric current plane and the smallest units forming a percolation network being the relatively close compacted aggregates ("segregated chain", proposed by Kusy [9]) instead of individual particles. L_ϕ and m_ϕ in this case were no longer concerned with individual particles, but described the geometry and orientation of V_2O_3 aggregates instead. The micrograph shown in Fig. 7b, in which fine particle aggregates distributed in polymer matrix are shown, may provide support for the above argument.

This argument may be also supported by the fact that the lowest L_ϕ and the highest m_ϕ values were obtained in the V_2O_3–PVC system formed by compaction sinter moulding. The lowest L_ϕ and highest m_ϕ values indicated that the percolation network was

5761

TABLE III Three-parameter fitting

Sample	σ_l^{-1} (Ω cm)	σ_h^{-1} (Ω cm)	t	ϕ_c	L_ϕ	m_ϕ	L_f	m_f	δ (%)
HDPE1	3.10×10^{10}	0.037	2.16	0.30	0.138	7.26	0.675	3.07	2.2
LLDPE1	1.35×10^{10}	0.037	2.47	0.32	0.132	7.58	0.726	3.65	2.5
LDPE1	4.26×10^{12}	0.037	2.78	0.38	0.137	7.32	0.777	4.48	2.2
EPOXY1	1.72×10^{12}	0.037	1.90	0.20	0.137	7.32	0.611	2.57	4.3
PVC1	8.38×10^{12}	0.037	2.77	0.10	0.036	27.6	0.673	3.06	1.3
HDPE2	2.26×10^{10}	0.092	2.32	0.28	0.119	8.40	0.688	3.20	1.4
LLDPE2	6.20×10^{10}	0.092	2.65	0.32	0.120	8.32	0.743	3.88	1.4

Note: The sample is named by the matrix material and a number, 1 = as-produced V_2O_3, 2 = ball-milled V_2O_3.
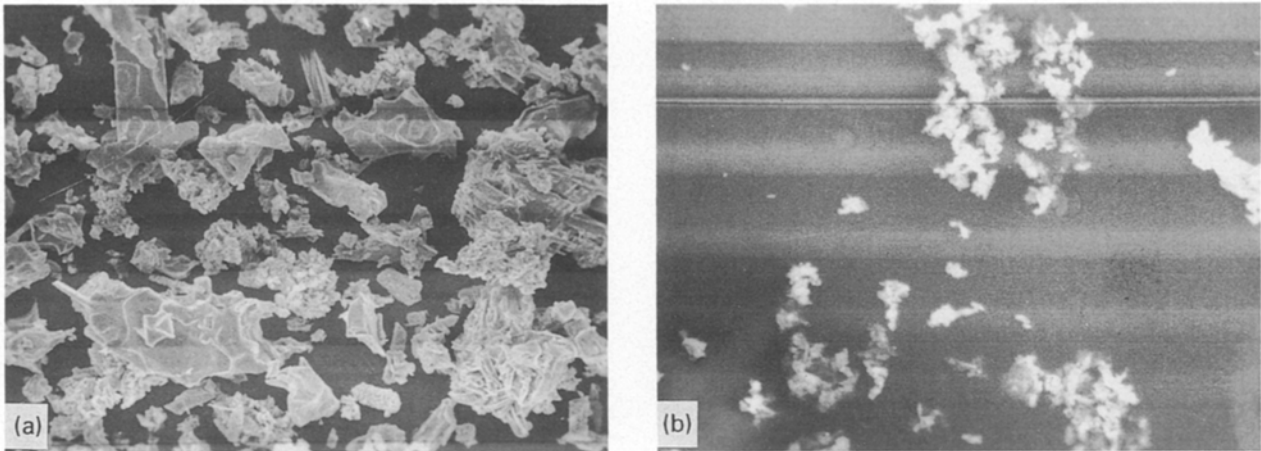

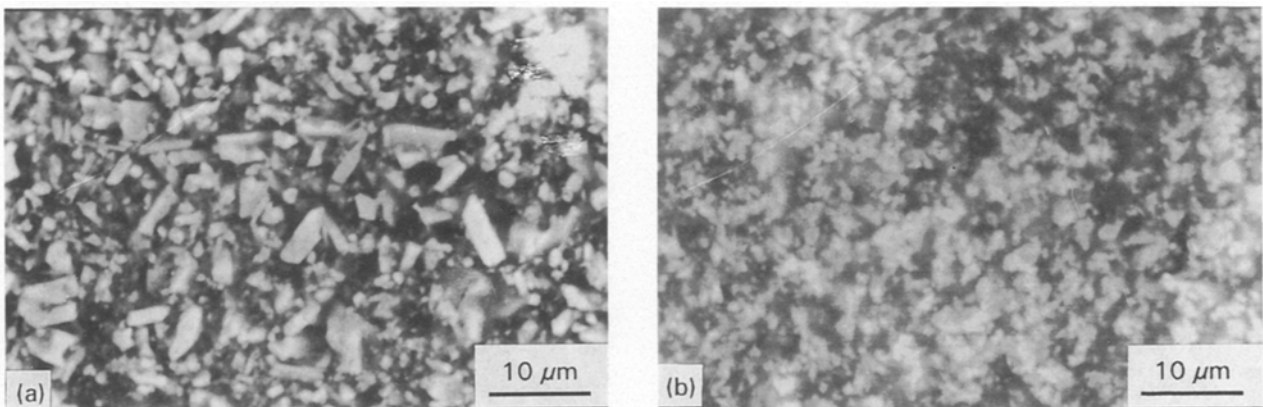Figure 6 SEM micrograph of V_2O_3 powder: (a) as-produced; (b) ball-milled.

Figure 7 SEM micrographs of V_2O_3–polymer composites. (a) Particles in V_2O_3–HDPE (V_2O_3 as-produced); (b) aggregates in V_2O_3–HDPE (V_2O_3 ball-milled); (c) polymer wetting of V_2O_3 in V_2O_3–HDPE (V_2O_3 as-produced).

formed mainly by layers lying in the current plane. The layers were formed by fine V_2O_3 particles wrapping around PVC grains during dry mixing and oriented by hot-pressing. This again showed that L_ϕ and m_ϕ were related only to the geometry and orientation of the smallest unit forming the percolation network. The unit could be individual particles or aggregates, or both, depending on the particle size and the mixing method used.

L_f values (effective demagnetization constant of polymer matrix) are also listed in Tables II and III. L_f values for various matrices were all greater than 0.6,

far greater than 1/3. The effective geometry of polymer matrices, according to L_f values, should be ellipsoids perpendicular to the electric current plane. The real situation, according to mixing methods, was that polymer matrices formed a connected network in three dimensions. Some portions of the network were arranged almost perpendicular to the electric current plane, hindering conductive particles from contacting, the rest may have been approximately parallel to that plane. The former portion was predominant since L_f was far greater than 1/3. This situation could possibly be produced by the fact that the high temperatures at which shear milling and hot-pressing were performed allowed the polymer to flow easily and the polymer acted as a lubricant and combiner to V_2O_3 powders. The polymer network could easily be seen in the SEM study of morphologies. Fig. 7c shows part of a typical polymer network with V_2O_3 particles and aggregates inside. The neighbouring V_2O_3 particles were in contact with each other and the polymer network crossed the whole medium.

It may be concluded that the effective demagnetization constant, L (L_ϕ or L_f), is due only to the geometry and the orientation of one component. For most cases the geometry and orientation are not regular, L can reflect to what extent the component may be avoided by electric current. $L = 1$ means that the component is not avoided at all by the electric current. $L = 0$ means that the component can be completely avoided by the electric current. $0 < L < 1$ means that part of the component is being avoided by the electric current. If the low-conductivity component cannot be avoided by the electric current (large L_f), then the conductive particles are separated by the low-conductivity component, contributing considerably to resistivity.

L may be further understood by answering why composites with the same V_2O_3 powder in different matrices have different critical volume fractions, shown in Fig. 4. From Table III it can be seen that different ϕ_c values related only to different L_f values. The largest ϕ_c value (0.380) in the V_2O_3–LDPE composite corresponded to the largest L_f value (0.77). This suggested that in these systems the geometry and orientation of the V_2O_3 powder was the same, but the extent to which the polymer matrix coated the V_2O_3 particles was different. LDPE coated V_2O_3 particles to the greatest extent (largest L_f), inhibited formation of the percolation network and increased the critical volume fraction of V_2O_3. Therefore, L_f appeared to give some information about the interaction between V_2O_3 and the polymer. It may be said that LDPE the best wetted the V_2O_3 particles, and that the interfacial energy of V_2O_3 particles coated by LDPE were the lowest.

Most t values in both Tables II and III were > 2, and were beyond the range of $t = 1.5$–1.6, deduced from percolation theory [11], but lay in the range of 1.5–2.8, obtained by Deprez and McLachlan [12] in their experiments on a series of flaky graphite particles undergoing compaction with polymer matrices. A large t gave a low rate of resistivity decrease with respect to the volume fraction change. As compared with L and m, the values of t were relatively diverse.

This again suggested that t was related to two components and was a characteristic parameter of the materials.

The critical volume fraction, ϕ_c, was also a materials characteristic parameter. It also depended on the geometries and orientations of two components, i.e. L_ϕ and L_f. According to Equation 3, L_ϕ and L_f affected ϕ_c differently. The difference may be more easily understood by the following equations, deduced from Equation 3

$$\frac{\partial \phi_c}{\partial L_\phi} = (1 - \phi_c) t \qquad (14)$$

$$\frac{\partial \phi_c}{\partial L_f} = \phi_c t \qquad (15)$$

ϕ_c is usually less than 0.5 and t is constant. Therefore, in the same system, the dependence of ϕ_c on L_ϕ is greater than that on L_f. But L_ϕ is a stable value and L_f is easily adjusted by altering the matrix and changing the mixing time and manner, so that the effect of L_f on ϕ_c is often considered (e.g. analysis of Fig. 4).

The GEM equation has proved to be a powerful tool to deal with the resistivity versus volume fraction in V_2O_3–polymer composites. Computer fitting of experimental data to the GEM equation can give property parameters, σ_l, σ_h, ϕ_c and t, component parameters L (L_ϕ and L_f) and random parameters m (m_ϕ and m_f), including almost all necessary information about property and geometry of individual components, arrangement manner and interaction between the two components.

5. Conclusions

1. A distinct insulator–conductor transition occurs at the critical volume fraction in V_2O_3–polymer composites. The critical volume fraction corresponds to the percolation threshold at which the percolation path formed by the V_2O_3 powder just crosses the medium.

2. The volume fraction dependence of resistivity obtained experimentally could be fitted by a computer program to the GEM equation to an acceptable accuracy. Variable parameters, including σ_l, σ_h, ϕ_c and t, could be provided by the fitting of data, L and m could be obtained by simple calculation.

3. Parameters L (L_ϕ or L_f) were related only to one component. L provided the effective geometry and orientation of the smallest electroconductive or insulating unit forming the percolation path or insulating network. This unit could be individual particles or particle aggregates (segregated chain) depending on the particle size and the mixing method. If $L < 1/3$, the effective unit may have had longer dimension along the electric current.

4. Exponent t defined a rate at which the resistivity decreased with an increase in the volume fraction of the conductive filler; t is a composite property characteristic and is related to the geometry and arrangement of two components.

5. The critical volume fraction was also a composite material characteristic and was related to two components.

References

1. M. Q. ZHANG and H. M. ZENG, *Engng. Plast. Appl.* (Chinese) **2** (1991) 50.
2. G. DENTSCHER, A. KAPILULNIK and M. RAPPAPORT, *Ann. Israel Phys. Soc.* **5** (1983) 207.
3. H. Y. SU, *Appl. Chem.* (Chinese) **7** (1990) 97.
4. K. A. HU, J. RUNT, A. SAFARI and R. E. NEWNHAM, *Ferroelectrics* **68** (1986) 115.
5. Y. PAN and GUO ZHANG WU, *J. Zhejiang Univ.* (Chinese) **4** (1994) 613.
6. D. A. G. BRUGGEMAN, *Ann. Physics Lpz.* **24** (1935) 665.
7. R. LANDAUER, *J. Appl. Phys.* **23** (1952) 779.
8. D. S. McLACHLAN, *J. Phys. C: Solid State Phys.* **20** (1987) 865.
9. R. P. KUSY, *J. Appl. Phys.* **48** (1977) 5301.
10. S. K. BHATTACHARYA, *J. Appl. Polym. Sci.* **25** (1980) 111.
11. R. ZALLEN, "The physics of amorphous solids", Ch. 4 (Wiley, New York, 1983).
12. N. DEPREZ and D. S. McLACHLAN, *J. Phys. D: Appl. Phys.* **D21** (1988) 101.